MJFAS Malaysian Journal of Fundamental and Applied Sciences
ISSN:2289-5981 e-ISSN:2289-599X
UTM UNIVERSITI TEKNOLOGI MALAYSIA

Vanadium oxides doped porous titania photocatalysts for phenol photodegradation

Khaw Swee Por[1], Ooi Yee Khai[1], Siew Ling Lee[2]*

[1]*Department of Chemistry, Faculty of Science, Universiti Teknologi Malaysia, 81310 UTM Johor Bahru, Johor, Malaysia.*
[2]*Centre for Sustainable Nanomaterials, Ibnu Sina Institute for Scientific and Industrial Research, Universiti Teknologi Malaysia, 81310 UTM Johor Bahru, Johor, Malaysia.*

Article history :
Received 7March 2016
Accepted 23 March 2016

GRAPHICAL ABSTRACT

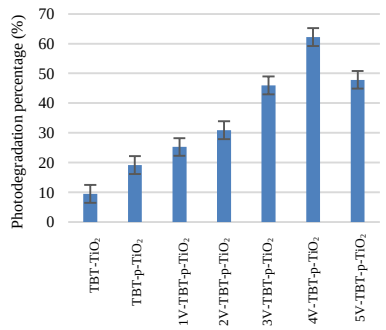

ABSTRACT

Vanadium oxides (1 - 5 wt%) doped porous TiO_2 using tetrabutyltitanate and cetyltrimethyl ammonium bromide as Ti precursor and template, respectively was successfully synthesized via sol-gel method. All the samples crystallined in anatase phase as indicated by X-ray diffraction analysis. The results of diffused reflectance UV-visible spectroscopy analysis showed that the band gap energy of TiO_2 reduced from 3.02 to 2.72 eV after introduction of 5 wt% V. The nitrogen adsorption-desorption analysis revealed that the surface area of samples increased with the amount of V dopant. These materials contained of disorder mesopores with particle size ranged 5 – 56 nm. Amongst, sample 4V-TBT-p-TiO_2 recorded the highest percentage of phenol degradation (62.2%) under visible light irradiation

Keywords: vanadium oxides, TiO_2, tetrabutyltitanate,cetyltrimethyl ammonium bromide

http://dx.doi.org/10.11113/mjfas.v12n1.407

1. INTRODUCTION

Phenol is the major component of water pollutant as it reacts with chlorine to form toxic polychlorinated phenolic compounds [1]. It is widely found in many industrial wastewater including resins, paint, oil refineries, herbicides, textile, food, flavoring agent, petrochemical, antioxidants and photographic chemicals [2]. Phenol is known as refractory organic compound which consists of carcinogenesis toxicity and mutagenicity [3]. European Union has categorized several phenolic compounds as primary contaminants [4].

Conventional wastewater treatment usually involves huge biological system which utilizes activated carbon, specific chemical or solvent to remove the phenolic compounds [5]. However, these methods have resulted high cost for further treatment of byproducts [6]. Therefore, an alternative way with a low cost and high efficient wastewater treatment method is highly desired to solve the problem.

Advanced Oxidation Processes (AOP) which utilizes photocatalysts to degrade organic pollutant into environmental friendly by products such as carbon dioxide, water and inorganic ions has been developed [7]. Titania-based photocatalytic oxidation appears as an effective method among AOP especially in mineralization of toxic and non-degradable organic pollutants in wastewater treatment [8,9]. TiO_2 is a good heterogeneous photocatalyst because it has high chemical stability, good thermal stability and relatively low cost.

Electron in the valence band of TiO_2 will excite to conduction band when it absorbs enough light energy. Thus, it results a positive vacancy or hole in the valence band. The photo-generated electrons and holes on the surface of catalyst function to transform the water molecule to hydroxyl radical. Then, the radicals will react with organic pollutants. Yet, the photo-generated electrons and holes may also recombine. Hence, the photoactivity of TiO_2photocatalyst can be improved by controlling the recombination rate of electrons and holes.

TiO_2 is not an effective photocatalyst under visible light irradiation due to its large band gap energy (3.2 eV). It causes TiO_2. Besides, the photocatalytic activity of TiO_2 has been limited by the fast electron-hole recombination. In order to enhance the photoactivity of TiO_2, modifications such as metal oxides doping [10], dye sensitization [11] and metal coupling [12] have been carried out. Amongst, metal oxide doping has attained the best result. However, there are contradict statements for photocatalytic

performance of metal oxide doped TiO_2. Some researchers reported doping of metal oxide could boost the photoactivity of TiO_2, but some other researchers denied it. Besides, the issue of low mass transport rates between the organic pollutant and the active central of TiO_2 is related to the porosity of TiO_2 [13].

In this study, vanadium oxide was doped into TiO_2 in order to delay the recombination of hole and electron pairs [14] and boost the adsorption activity [15]. Besides, porous TiO_2 was synthesized in order to further enhance the photocatalytic activity of TiO_2. The effects of weight percentage of V oxide dopant on the properties and photodegradation of phenol were explored.

2. EXPERIMENTS

2.1 Photocatalyst Preparation

Vanadium oxide doped porous TiO_2 was synthesized via sol-gel method. Amount of 8 mL of ethanol (99.98%, Qrex) was used to dissolve 0.0875g of cetyltrimethylammonium bromide (CTAB, 95%, Aldrich). Then, the reaction mixture was added with 2 mL of tetrabutyltitanate (97%, Aldrich) and 0.1 mL of 1M hydrochloric acid (37%, Aldrich). After that, amount 0.9 mL of distilled water and 4 mL of ethanol were further added in the reaction mixture. The reaction mixture was stirred for an hour at room temperature and labeled as solution A. Vanadium(V) oxide solution was prepared using ethanol (99.98%, Qrex) to dissolve vanadylacetylacetonate (98%, Aldrich. After that, the vanadium(V) oxide solution was added dropwise into solution A. The mixture of two solutions was further stirred for an hour at room temperature to ensure the homogeneity of solution. Next, a gel was formed and aged at room temperature for 24 hours. The gel was then dried at 353 K for 8 hours. Finally, the sample was grinded and underwent calcination process at 773 K for 3 hours. The sample was collected and marked as xV-TBT-p-TiO_2, where x referred to wt% of V ranging 1 – 5 wt%. For comparison, undoped porous TiO_2 was prepared with same procedure without the addition of V precursor. The sample was labeled as TBT-p-TiO_2. Besides, another undoped TiO_2 was prepared without usage of CTAB. The sample was labeled as TBT-TiO_2.

2.2. Characterizations

Characterizations of all the synthesized TiO_2-based photocatalysts were carried out. X-ray diffraction analysis (Bruker Advance D8 X-ray diffractometer) with Cu K_α radiation of λ= 1.5406 nm at 40 KV and 40 mA, scan rate of 0.1°/s in the range of 2θ = 20 - 60° was used to determine the phase and crystallinity of samples. The band gap energy of samples were determined using Diffused reflectance ultraviolet visible spectroscopy (Perkin Elmer Ultraviolet-visible Spectrometer Lambda 900) with barium sulfate as reference. Fourier transform infrared spectroscopy (FTIR-8300 Spectrophotometer) was utilized to detect the functional groups of synthesized TiO_2 samples. The surface area, type of pore and pore size of samples was determined by nitrogen adsorption-desorption analysis (Surfer, Thermo Scientific). Field emission scanning electron microscope (Hitachi SU8020) was used to investigate the morphology of TiO_2photocatalysts.

2.3 Photoatalytic testing

The photocatalytic activity of the synthesized samples was tested by photodegradation of phenol under visible light irradiation. Sample (0.1 g) was immersed and suspended in the phenol solution (50 mL) in the 100 mL beaker. The initial concentration of phenol solution was fixed at 50 ppm. The visible light source to irradiate the suspension was halogen fiber optic light illuminator (BOTE, 150 W). The solution was stirred for 2 hours in dark condition in order to establish adsorption equilibrium. The distance between the normal incidence of visible light and the solution was fixed at 25 cm. The solution was irradiated under visible light for 5 hours and filtered using a membrane syringe filter. UV-Vis Spectrophotometer (ThemoFisher, Genesys 10S) was used to measure the concentration of filtrate. The experiment was carried out three times for every samples.

3. RESULTS AND DISCUSSION

Fig. 1 indicates the XRD patterns of undoped TiO_2 and vanadium oxide doped TiO_2. All the samples exhibited similar peaks located at 2θ = 25.3, 37.9, 48.1, 54.1 and 55.2°. They are significant peaks for TiO_2 in anatase phase (JCPDS 21-1272). All samples crystallined in anatase phase even after calcination process at 773 K or with vanadium oxides doping. No characteristic peaks for vanadium oxide were found in the XRD patterns. It could be due to the vanadium oxide was either successfully incorporated in the lattice of TiO_2, or amount of vanadium oxide was very small to be detected. Alternately, the doped vanadium oxide maybe highly dispersed on the surface of TiO_2. The crystalline sizes of TiO_2 and vanadium oxide doped porous TiO_2 synthesized was ranging 13.23 - 19.82 nm. Vanadium doping did not cause significant change in crystalline size.

DRUV-Vis spectra of undoped TiO_2 and vanadium oxide doped TiO_2 are shown in Fig. 2. Undoped TiO_2 powder existed in white colour while vanadium oxide doped TiO_2 powder was grey in colour. The colour intensity of vanadium doped porous TiO_2 increased with the increasing amount of doped vanadium in the samples. A shoulder band at 230 - 280 nm and an absorption peaks at around 290 - 350 nm were found in undoped TiO_2 samples. Their formation was detected due to the charge transfer from O^{2-} to the tetrahedral Ti sites and octahedral Ti sites, respectively [16]. The red-shift phenomenon was clearly observed in the series of V-TBT-p-TiO_2 samples compared to TiO_2. The higher the amount of vanadia doping, the greater the red-shift was [17].The peak shifting

around 390 nm and formation of new absorption peak were caused by doping of vanadium oxides. The abilities of samples to absorb the photon energy in the range of 400 – 800 nm was indicated by the absorption curves tailing of vanadium oxide doped porous TiO_2 samples. According to previous studies, it was reported that V^{5+} has an absorption peak at < 579 nm, while V^{4+} has an absorption peak at around 770 nm [18,19]. Additionally, the tailing of absorption band also resulted from the charge-transfer transition from the d-orbital of V^{4+} to the conduction band of TiO_2 [20].

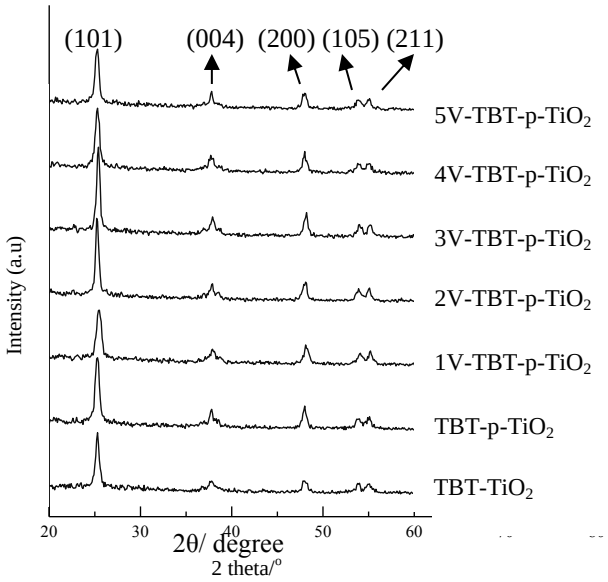

Fig. 1 XRD patterns of undoped TiO_2 and vanadium oxide doped TiO_2

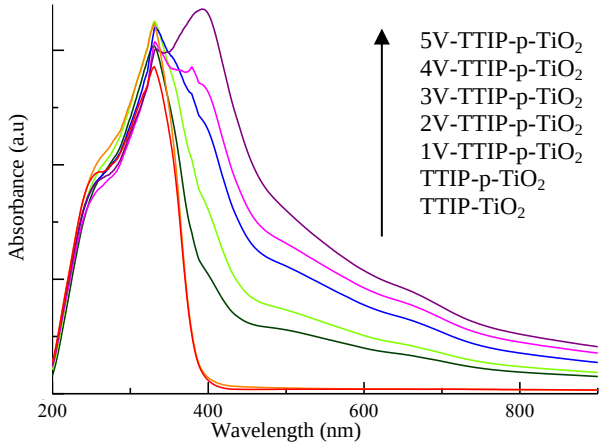

Fig. 2 DRUV-VIS spectra of undoped TiO_2 and vanadium oxide doped TiO_2

The band gap energy of undoped porousTiO_2 and vanadium oxide doped porous TiO_2 are shown in Table 1. The increasing amount of vanadia caused significant drop in the band gap energy of TiO_2. 5V-TBT-p-TiO_2 records the lowest band gap energy of 2.66 eV. It was believed that doping vanadium oxides into TiO_2 has created new lower energy levels between the valence band and conduction band of TiO_2. It was previously reported that the 3d orbital of vanadium helped to reduce the band gap of TiO_2, thus extending the wavelength of the vanadium oxide doped porous TiO_2 into the visible light region [21].

Table 1 Band gap energy, BET surface area and pore size of samples

Sample	Band gap energy (eV)	BET surface area (m^2/g)	Average diameter of pore size (nm)
TBT-TiO_2	3.02	34	6.20
TBT-p-TiO_2	3.11	15	18.14
1V-TBT-p-TiO_2	2.85	22	7.42
2V-TBT-p-TiO_2	2.79	20	10.52
3V-TBT-p-TiO_2	2.76	26	6.84
4V-TBT-p-TiO_2	2.72	29	6.36
5V-TBT-p-TiO_2	2.72	37	5.60

Nitrogen adsorption-desorption analysis showed that the surface area of TiO_2 with CTAB (TBT-p-TiO_2) was lower than TiO_2 without CTAB (TBT-TiO_2) which were 15 and 34 m^2/g, respectively (Table 1). The usage of CTAB as template could have slowed down the rate of hydrolysis as CTAB might compete with TTIP for hydroxyl group. When the hydrolysis rate decreased and the rate of condensation increased, the number of Ti-O-Ti linkage increased. The particle growth mechanism altered from cluster-cluster to monomer-cluster [22]. Therefore, more branched structures were formed, which lowered the surface area of sample. As shown in Table 1, the BET surface area of vanadium doped TiO_2 increased with the amount of V dopant. Amongst, sample 5V-TBT-p-TiO_2 recorded the highest surface area of 37 m^2/g. Usually, the pore size of samples is closely related to the surface area. The smaller the pore size, the higher the BET surface area is [23]. As a result, the 5V-TBT-p-TiO_2 sample had the smallest average pore size among the samples which was 5.60 nm with the highest BET surface area detected.

Fig. 3 demonstrates the nitrogen adsorption-desorption isotherms of undoped porous TiO_2 and vanadium oxide doped porous TiO_2. According to the new isotherms classification by Donohue and Aranovich, the isotherms of samples were of type (IV) with type (III) like hysteresis loop [24], indicating presence of mesopores in the samples. The mesopores could be resulted from the particle agglomeration induced by calcination at high temperature and thus it is in disordered form. The presence of upward inflection in isotherm graph at P/P_o= 1 showed the presence of macropores in the samples. The hysteresis loops of samples were consisting of slit shape pores with

uniform (Type H_4) and non-uniform (Type H_3) sizes according to IUPAC classification [25].

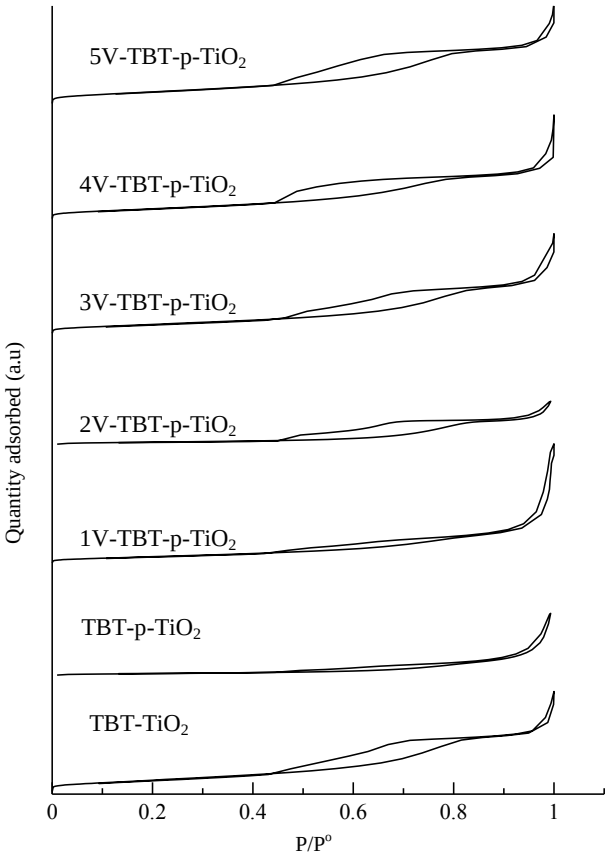

Fig. 3 Nitrogen absorption-desorption isotherms of undoped TiO_2 and vanadium oxide doped TiO_2

The FTIR spectra of TiO_2 and vanadium oxide doped porous TiO_2 are illustrated in Fig. 4. The stretching vibration mode of hydroxyl group located at around 3440 cm^{-1}, while the peak at 1630 cm^{-1} indicated the presence of the bending vibration mode of hydroxyl group. It was found in every calcined photocatalysts which was corresponded to the hydroxyl group and surface-absorbed water. The peak for vibration modes of O-Ti-O bond located at 569-646 cm^{-1}. The results indicated that no peaks shifting were detected. There was no significant sharp peak of the O=V=O stretch in V_2O_5 at 1021 cm^{-1} [26]. This supports the XRD results that the vanadia was successfully incorporated within the TiO_2. CTAB template was completely removed after calcination process at 773 K as there were no stretching bands of methylene and methyl groups found at around 3000-2800 cm^{-1}.

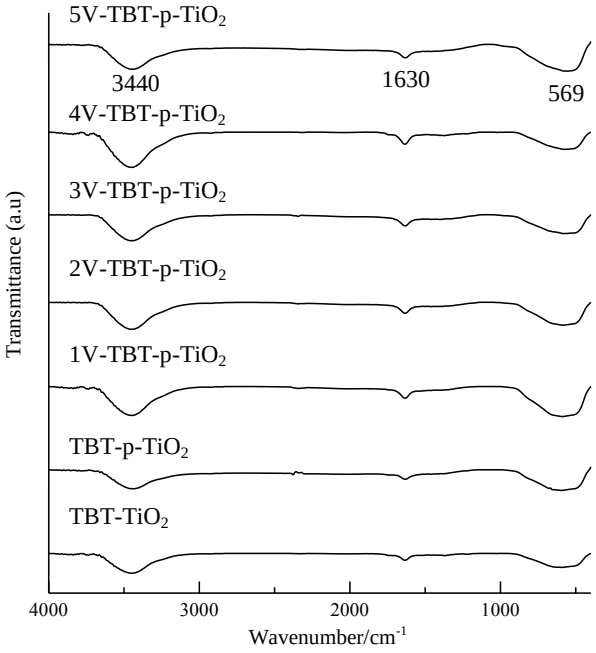

Fig. 4 FTIR spectra of undoped TiO_2 and vanadium oxide doped TiO_2

Fig. 5 shows the FESEM micrographs of undoped TiO_2 and vanadium oxide doped porous TiO_2. As can be seen, the morphologies of samples with CTAB as template present anomalistic sphericity, while sample without CTAB did not [27]. The spherical shape formation of TiO_2 was due to addition of CTAB template. The particle size of all TiO_2 synthesized was ranged from 5 – 56 nm (Fig. 6). It was found that most of the resulted TiO_2 photocatalysts had the particle size which was ranged between 11 – 24 nm. Thus, the results are well matched with the crystallite size calculated via Scherrer's equation (12.53–18.33 nm).

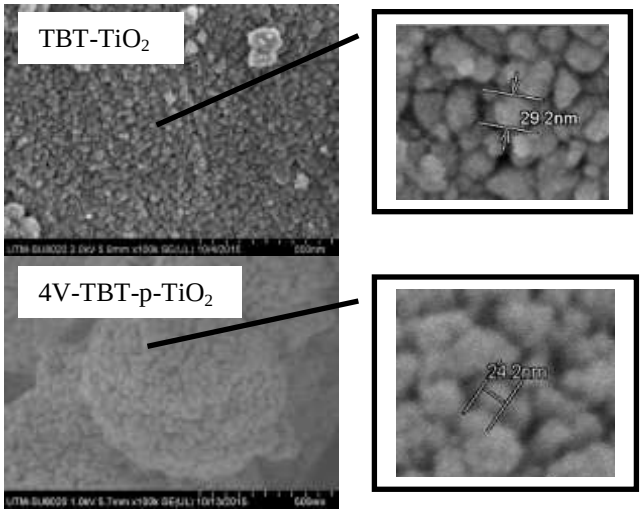

Fig. 5 FESEM images of undoped TiO_2 and vanadium oxide doped TiO_2

Photocatalytic performance of undoped porous TiO_2 and vanadium oxide doped porous TiO_2 samples was evaluated through phenol photodegradation under visible light (Fig. 6). The results indicated the undoped TiO_2 has the poorest activity as it only photodegraded 9.2% phenol after 5 hours of reaction. The photocatalytic activity of the samples increased with increased amount of vanadia dopant up to 4 wt%. It was followed by a decrease in rate with further increase in vanadia amount. Amongst, 4V-TBT-p-TiO_2 showed the highest degradation percentage of 62.2%. The results may imply the importance of both porosity and V dopant for the enhanced photocatalytic performance.

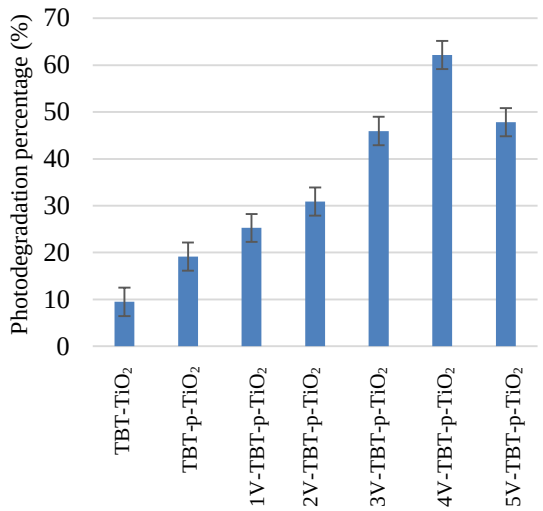

Fig. 6 Photodegradation percentage of undoped TiO_2 and vanadium oxide doped TiO_2

Doping of vanadia into TiO_2 could improve the electron-hole separation process. This phenomenon occurred due to vanadia doping favors the migration process of photogenerated electrons to vanadium. Vanadia clusters functions as a separation center at low concentration. Thus, the photogenerated electrons were transferred from TiO_2 conduction band to the dopingvanadium species and the holes accumulate in the TiO_2 valence band. As a result, photogenerated electrons and holes were efficiently separated. However, vanadia clusters might have acted as a recombination center at a higher concentration of 5 wt%. The recombination rate between electrons and holes increased directly with the increased of vanadia amount. The increasing of vanadia clusters in titania could decrease the average distance between trap sites, leading to high electron-hole recombination rate [28]. Additionally, the active site of TiO_2 would be shielded when there were too many vanadia clusters in TiO_2. Hence, it would increase the turbidity of the system and subsequently decreased the concentration of the electrons on the surface and holes available for further reactions.

4. CONCLUSION

Vanadium oxides (1 - 5 wt%) doped porous TiO_2 using TBT as Ti precursor was successfully synthesized via sol-gel method. CTAB was used as template and it was completely removed after calcination process. All samples crystallined in anatase phase with crystalline size ranged 12.53 - 19.82 nm. Doping of vanadium oxide had significantly reduced the band gap energy of porous TiO_2 from 3.02 eV (TBT-TiO_2) to 2.72 eV (5V-TBT-p-TiO_2). The photocatalytic activity of the samples increased with increased amount of vanadia dopant up to 4 wt%, followed by a decrease in photoactivity when further increment in the amount of vanadium. It has been demonstrated that both porosity and V dopant are crucial to improve the photocatalytic activity of TiO_2. Sample 4V-TBT-p-TiO_2 exhibited the highest photocatalytic percentage for phenol degradation among the samples which was 62.2%.

ACKNOWLEDGEMENTS

The authors gratefully acknowledge the Ministry of Higher Education (MOHE), Malaysia and Universiti Teknologi Malaysia (UTM) for the financial supports through Research University Grant (Vote No. (Q.J130000.2426.03G35). Khaw Swee Por acknowledges the financial support provided from UTM in the form of Research Student Grant (RSG).

REFERENCES

[1] Y.K. Ooi, L. Yuliati, S.L. Lee, Jurnal Teknologi. 69:5 (2014) 81-86
[2] O. B. Ayodele, J. K. Lim, B. H. Hameed, Chem. Eng. J. 197 (2012) 181–192.
[3] J. Matos, J. Laine, Herrmann, J. Appl. Catal. B: Environmental. 18 (1998) 281-291.
[4] Y.K. Ooi, L. Yuliati, S.L. Lee, Adv. Mater. Res. 1109 (2015) 424-428
[5] R. L. Autenrieth, J. S. Bonner, A. Akgerman, E. M. McCreary, J. Hazardous Materials. 28 (1991) 29–53.
[6] C. Hu, Y. Z. Wang, H. X. Tang, Chemosphere. 41 (2000) 1205–1209.
[7] M. Ziegmann, F. H. Frimmel, Water Sci Technol. 61 (2010) 273–281.
[8] N. Barka, S. Qourzal, A. Assabbane, A. Nounah, Y. Ait-Ichou, Arab. J. Chem. 3 (2010) 279-283.
[9] Pei Wen Koh, Leny Yuliati, Hendrik O. Lintang, Siew Ling Lee, Aust J. Chem. 68 (2015) 1129-1135
[10] J. Choi, H. Park, M. R. Hoffmann, J. Phys. Chem. C. 114 (2010) 783-792.
[11] P. Chowdhury, J. Moreira, H. Gomaa, A. K. Ray, Ind. Eng. Chem. Res. 51 (2012) 4523–4532.
[12] A. H. Zyoud, N. Zaatar, I. Saadeddin, C. Ali, D. Park, G. Campet,H. S. Hilal, J. Hazard. Mater. 173 (2010) 318–325.
[13] X. D. Wang, R. A. Caruso, J. Mater. Chem. 21 (2011) 20-28.
[14] H. Hamdan, M. N. M. Muhid, S. L. Lee, Y. Y. Tan, Int. J. Chem. React. Eng. 7 (2009) Article 54.
[15] X. L. Liang, S. Y. Zhu, Y. H. Zhong, J. X. Zhu, P. Yuan, H. P. He, J. Zhang. Appl. Catal. B: Environmental. 97 (2010) 151-159.
[16] E. Astorino, J. B. Peri, R. J. Willey, G. J. Busca, Catal. 157 (1995) 482- 500.
[17] C. S. Jeffrey Wu, C. H. Chen, J. Photoch. Photobio. A: Chemistry. 163 (2004) 509–515.

[18] R. Asahi, T. Morikawa, T. Ohwaki, K. Aoki, Y. Taga, Science. 293 (2001) 269-271.
[19] K. Bhattacharyya, S. Varma, A. K. Tripathi, S. R. Bharadwaj, A. K. Tyagi, J. Phys. Chem. C112 (48) (2008) 19102-19112.
[20] K. Nagaveni, M. S. Hegde, G. Madras. J. Phys. Chem. B. 108 (52) (2004), 20204–20212.
[21] A. L. Manoj, V. Shaji, S. N. Santhosh, Catal.2 (2012) 572-601.
[22] S. Katalin, Mater.3 (2010) 704-740.
[23] T. B. Nguyen, M. J. Hwang, K. S. Ryu, Appl. Surf. Sci. 258 (2012) 7299-7305.
[24] M. D. Donohue, G. L. Aranovich, Fluid Phase Equilibr. 158–160 (1999) 557–563.
[25] K. S. W. Sing, D. H. Everett, R. A. W. Haul, L. Moscou, R. A. Pierotti, J. Rouquerol, T. Siemieniewska, Pure Appl. Chem. 57(4) (1985) 603-619.
[26] K. Bhattacharyya, S. Varma, A. K. Tripathi, S. R. Bharadwaj, A. K. Tyagi, J. Phys. Chem. C112 (48) (2008) 19102-19112.
[27] W. C. Lin, Y. J. Lin, Environ. Eng. Sci. 29 (2012) 447-452.
[28] F. B. Li, X. Z. Li, Chemosphere. 48 (2002) 1103.